

**LOW CYCLE FATIGUE CHARACTERISTICS OF BRIDGE DECK RC SLABS  
UNDER THE REPETITION OF WHEEL LOADS**

(Rearrangement in English of paper in Proceedings of the Japanese Society of Civil Engineers, Vol.390/V-8, Feb., 1988)



Keiichiro SONODA



Toshio HORIKAWA

**SYNOPSIS**

A total of 47 model slabs whose scale was about 1/3 to a typical deck panel between adjacent main girders of an existing steel-concrete composite girder bridge in Japan were tested under the repetition of a wheel load using a wheel tracking machine originally developed by Osaka City University. The tests were confined with a low cycle fatigue range in which the repetition of a wheel load was less than  $2 \times 10^4$  times. Numerous data obtained in the tests are used to reveal the low cycle fatigue characteristics of bridge deck RC slabs. Besides, assuming that such characteristics may also significantly control the high cycle characteristics of the slabs, a method for estimating fatigue strength and fatigue life of bridge deck RC slabs is proposed.

---

K.Sonoda is a professor of civil engineering at Osaka City University, Osaka, Japan. He received his Doctor of Engineering Degree from Osaka City University in 1976. His research interests mainly cover ultimate loading capacities and fatigue strengths of reinforced concrete slabs and steel-concrete composite slabs. Recently, he studies dynamical behaviors of RC members and composite slabs. He and his coauthor were awarded a JSCE prize (Yoshida Prize) in 1989 for a study of present paper. He is a member of JSCE, JCI and ASCE.

---

T.Horikawa is an associate professor of civil engineering at Osaka Institute of Technology, Osaka, Japan. He received his Doctor of Engineering Degree from Osaka City University in 1984. His research interests include elastic problems of thick plates, fatigue properties of prototype's RC slabs and composite slabs under a wheel tracking equipment of large scale size with rear double tires or a tire of the so-called Jumbo jet plane. He is a member of JSCE and JCI.

---

## 1. INTRODUCTION

Since it was started to recognize the problem of cracking damage of bridge deck RC slab in the earlier 1960's in Japan, many engineers and research workers have studied this problem. The authors were first interested in the problem in about 1975, and have made some of experimental and theoretical studies [2-5]. The most important result obtained in these studies is that cracking damage of RC slabs is a kind of fatigue in a broad sense and it is caused by repetitive and moving loads by traffic vehicles. In design of RC slabs based on the allowable tensile stresses of reinforcement, an effect by the movement of wheel load was usually considered under estimations of the maximum bending moment by means of various influence surfaces about moments.

Since mechanical response of cracking slab is not linear, the moving of load induces the fluctuating action of combined stresses, and it makes crack lengths enlarge and crack faces rub out. Therefore, it should be pointed out that cracking slabs might collapse under a considerably low intensity of wheel load, because of the degradation of shear resistance of slab which is mainly relying on the interlocking of concrete aggregate. As such a knowledge is only qualitative, however, further researches need to quantify it for contributing to a design method [5,6].

In this paper, for the purpose of revealing the process of cracking damage of RC slabs, 47 model slabs whose scale was about 1/3 to a typical deck panel between adjacent main girders of an existing steel-concrete composite girder in Japan were tested. For simulating the repetitive loading of traffic vehicles, a wheel tracking machine originally developed by Osaka City University was used. The tests were confined with a low cycle fatigue range in which the repetition of wheel tracking was less than  $2 \times 10^4$  times.

We examined several relations among magnitude of wheel load, repetition cycle of tracking, thickness of slab and arrangement of reinforcements under considerations of progress of cracks, variation of stresses of reinforcements and increase of deflections et al.. We propose an reasonable estimation of fatigue life in road bridge deck RC slabs by surly observing some results obtained from our experiments, because a cracking damage of slabs is mainly governed by degree of tracking cycle of the over-loaded wheel vehicle.

## 2. LOW CYCLE FATIGUE TEST OF RC SLABS

### 2.1 Wheel Tracking Machine and Model Slabs

An outline of testing equipment is shown in Figure 1 and 2. Figure 1 is a whole appearance, and the test slabs are simply supported at all edges. In order to hold a wheel load intensity constant, a counter weight system was used in an early stage (1982-1985). But this system is restricted in accuracy to control a constant wheel load. Lately (1985-1986), therefore, an electrical hydro-servo system was used to control the wheel load. By this system, the control of a constant wheel load was remarkably improved (see Figure 3). In addition, an automatic operation and measurement could be performed with the aid of computer (see Figure 2). Furthermore, moving speed of wheel load was about 10 m/min.

The details of the test slabs are listed in Table 1. Slabs NOS, NOR and NWR were tested by the servo control method. All reinforcements of the slabs were D6 (deformed bar with 6mm in diameter), and rolled out from coiled wire. The strengths of concrete and re-bar is shown in Table 2. Although the concrete was placed in the same design mix proportion (Table 3), the strengths of test

cylinders considerably varied depending on the time of casting. Design Value of slab thickness was 70mm, but it was finished as shown in Table 1.

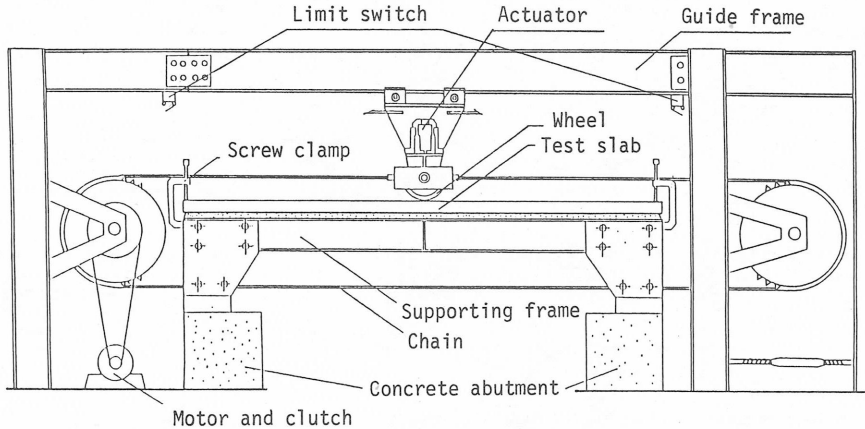


Figure 1 General view of test apparatus

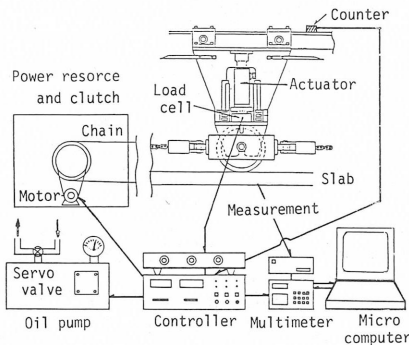


Figure 2 Hydro-servo loading and micro computer measurement systems

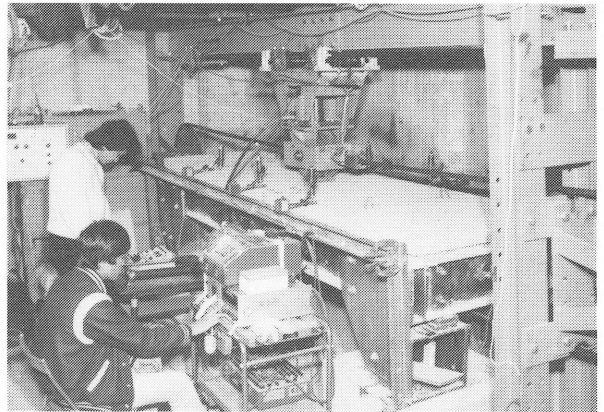


Photo 1 Test view

## 2.2 Method of Experiments and Loading Programs

Figure 3 shows variation of constant wheel load to be established in both systems. It was difficult for the first system to keep a standard value to be controlled, because this system was directly influenced by an inertia of counter weight and a viscosity of jack oil which flowed through gum-pipes. The rate of variation in counter weight system were  $\pm 10\%$  in a lower load level and  $\pm 20\%$  in a higher level, difference in hydro-servo system was less than 5%.

Figure 4 shows the supporting system of test slabs and the tracking zone of wheel. The shorter span is 80cm, the longer span is 3m, and this aspect ratio may regard them as a one-way slab. The wheel tracking zone is central 2.3m. The contact area of wheel, covered by a polyurethane-gum of thickness 20mm, to slab surface increases in proportion to load level. In a lower load level (16.7kN) it was 15cmx3cm, in a higher load level (54.9kN) 15cmx5cm, and in the highest load level near the collapse load in static test about 15cmx8cm.

If the test slabs are regarded as a model of highway RC slabs, a corresponding design load according to the Standard Specifications of Highway Bridge in Japan can be defined as a load inducing the maximum stress of main reinforcement equal to the allowable tensile stress ( $\sigma_{sa}=137\text{MPa}$ ). Calculating the corresponding design load ( $P_d$ ) by a thin elastic plate theory and an ordinary equation for RC beams,  $P_d=20.6\text{kN}$  in test slab ISS,  $P_d=15.7\text{kN}$  in NWR, and in the other slabs  $P_d=16.7\text{kN}$  are obtained.

Table 1 Dimensions of test slabs

Name	Num-ber	Size (mm×mm)	Dept (mm)	Effective depth(mm)		Spacing of bottom (mm)		Spacing of top bar(mm)	
				Main	Distr.	main	Distr.	main	Distr.
IS	6	900×3100	72	62	56	50	50	—	—
ISS	6	"	75	65	59	50	50	—	—
IR	6	"	72	62	56	50	50	100	100
ID	6	"	"	"	"	50	50	50	50
OS	4	"	"	"	"	50	100	—	—
OR	3	"	"	"	"	50	100	100	200
NOS	4	"	70	60	54	50	70	—	—
NOR	8	"	"	"	"	50	70	100	140
NWR	4	1100×3100	"	"	"	50	70	100	140

Table 2 Strengths of concrete and reinforcement bar

Test Slab	Re-bar(D6)		Concrete		Age / Casting
	Yield point(MPa)	Tens. str- ength(MPa)	Comp. str- ength(MPa)	Tens. str- ength(MPa)	
IS, IR, ID OS, OR	363*	559*	46.9	3.6	70 days on Aug.
ISS	467	632	19.4	1.9	28 days on Mar.
NOS, NOR	373	539	21.7	2.1	28 days on Nov.
NWR	373	539	22.7	2.1	28 days on Sep.

Note) \* annealed

The magnitude of wheel load in fatigue test was set by multiplying  $P_d$  by a certain coefficient  $\mu(\mu>1)$ . The repetitive cycles of wheel tracking were set in the range of 1-2x10<sup>4</sup>. When the collapse did not occur within this range, test was continued up to collapse, after the magnitude of load increased step by step.

### 2.3 Results of Test

#### a) Static test

In static tests, all slabs collapsed in a punching shear mode. Since collapsed area was limited to the vicinity of three loading points, center of slab and two points of ±90 cm apart from center, the tests were carried out three times for each slab at different loading points. The collapse loads obtained are listed in Table 4. An example of collapse mode is illustrated in Figure 5. Initial crack occurred parallel to distribution reinforcements in the bottom surface of slab beneath a loaded portion, and it propagated along reinforcements. Load when the first crack was observed with the naked eyes, was 19.6kN in test slab ISS, 9.8kN in NOR and NWS, 14.7kN in the other slabs. Load-deflection curves at the slab center are shown in Figure 6. Assuming that tensile concrete of section is valid, theoretical deflection by thin plate elasticity, elastic modulus 19.6GPa, under the design equivalent load ( $P_d$ ) is 0.28-0.31mm for the slab shown as symbol① in Figure 6. Assuming that tensile concrete of section is invalid, it is about 3 times as large as them shown as symbol②.

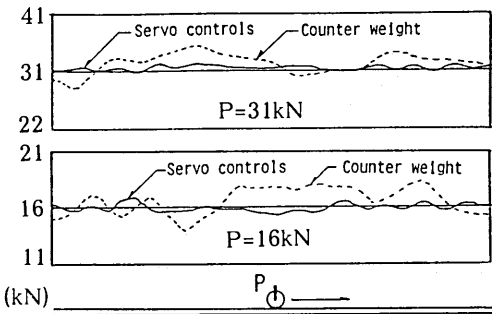


Figure 3 Variation of wheel load

Table 3 Mix proportion of concrete

Max aggreg- ate size(mm)	Slump (cm)	Air Con- tent (%)	W/S (%)	s/a (%)	Cement factor (kN/m³)
15	10~22	3~5	50	47	3.6

Note) \* 10mm in only test slab ISS

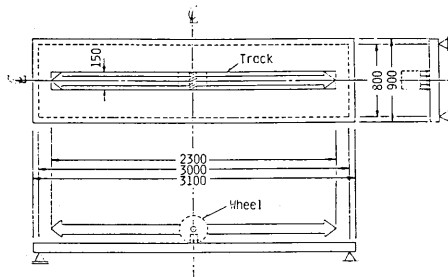
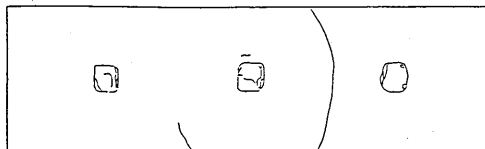


Figure 4 Wheel tracking zone

Top Surface



Bottom Surface

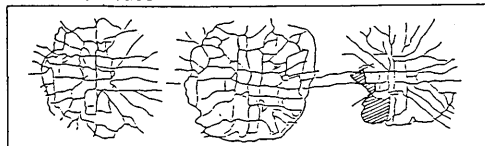


Figure 5 Static collapse mode (slab ISS)

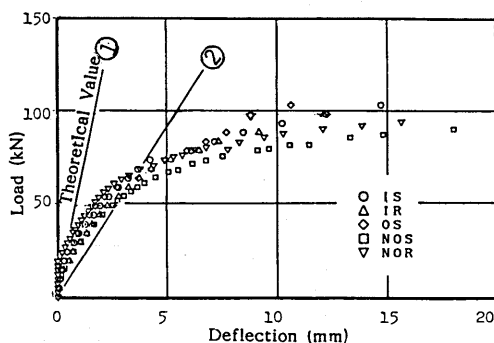


Figure 6 Deflection at the center of slab

Table 4 Static collapse load

Slab	Collapse Load (kN)				Calculated Value*
	+90cm	Center	-90cm	Mean	
IS	104	108	103	104	130
IR	98	103	101	101	130
ID	116	122	127	122	130
OS	99	103	99	100	122
OR	76	76	77	76	122
ISS	129	132	140	135	84
NOS	94	95	89	93	81
NOR	96	97	99	92	81
NWR	98	93	92	94	83

Note) \* calculated by punching shear formula in the Standard Specification of Japan

## b) Wheel Tracking Test

### (1) Fatigue strength

The results of wheel tracking fatigue test for total 35 test slabs are summarized in Table 5. In this Table, numerals marked \* are the data obtained after the repetition of 1-2x10<sup>4</sup> times of lower loads than collapse load. The relationship between collapse load and fatigue life is shown in Figure 7. In this figure, the ordinate shows the ratio of wheel load to static collapse load. By reason of large scattering, it is difficult to find quantitative conclusions from Figure 7 and Table 5. But, the followings may be pointed out:

- 1) The fatigue strength of slab ISS with 75mm thick is considerably larger than that of slab IS with 72mm thick. It can, therefore, be mentioned that the fatigue strength and life are significantly influenced by slab thickness.
- 2) Slabs IR, OR, ID, NOR, NWR with top reinforcements are more weak in fatigue strength than slabs IS, ISS, OS, NOS without them.
- 3) Between slab NOR with the shorter span of 80cm and NWR with the longer span of 100cm, a difference can not be appreciable.

Table 5 Fatigue strength and life

P (kN)	Slab								
	ISS	IS	IR	ID	OS	OR	NOS	NOR	NWR
49 $\Delta^1$	5155	195	126	369	538	—	—	—	—
44	5522 10723 17061 19297	1238	—	—	1231	—	—	—	—
39	—	970 2134	165	—	5491	87	—	—	—
34	(*)5	12401	291	599	—	—	—	—	—
29	(*)1	—	2029 1306	2150 5718 392	—	—	3628 1842	2345 2455 6435	168
25 $\Delta^2$	(*)2	—	(*)7	(*)9	—	1084	7415	1775 2409	3000
20 $\Delta^3$	(*)3	—	—	—	—	—	(*)11	(*)13 (*)14	—
17 $\Delta^4$	—	(*)6	—	(*)8	—	—	(*)10	(*)12 (*)14	—

Note)  $\Delta^1$  : 51.0kN in IS  $\Delta^2$  : 23.7kN in NWR, 25.5kN in ISS  
 $\Delta^3$  : 21.6kN in ISS  $\Delta^4$  : 15.7kN in NWR  
 \* 1~14 : Test results after the repetition of  $1 \times 10^4 \sim 2 \times 10^4$  of  
 a load circled with ○

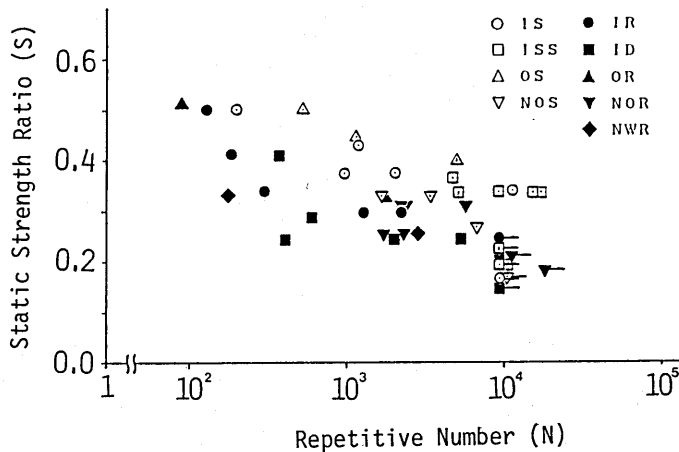


Figure 7 Fatigue strengths and lives in wheel tracking tests

## (2) Cracking and collapse mode

Cracking pattern and collapse mode were similar among all the test slabs. For example, in slab NOS without top reinforcements under  $P=24.5\text{kN}$ , they are shown in Figure 8. Initial cracks caused by concrete-shrinkage were slightly observed on the bottom surface of slab. When a wheel load was first placed at the center of slab, cracks were developed along main and distribution reinforcements as shown in Figure 8. By repeatedly tracking of a wheel load, cracks spread over the whole area of the bottom surface of slab. In an early stage, the cracks were very small so that they disappeared after unloading. At repetitive number  $N=3000$  of wheel tracking, cracks parallel to main reinforcements were also observed on the top surface of slab. Then the slab collapsed at  $N=7,415$ .

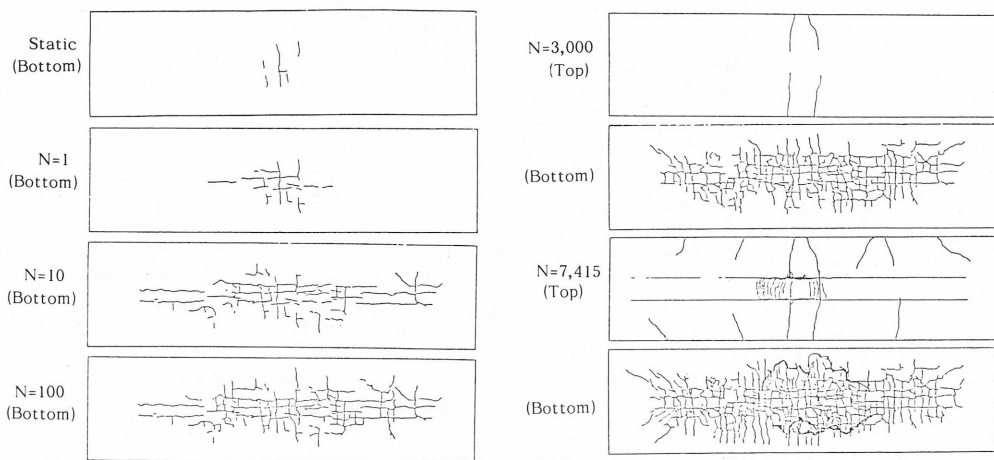


Figure 8 Cracking pattern and failure mode of slab NOS in  $P=24.5\text{kN}$

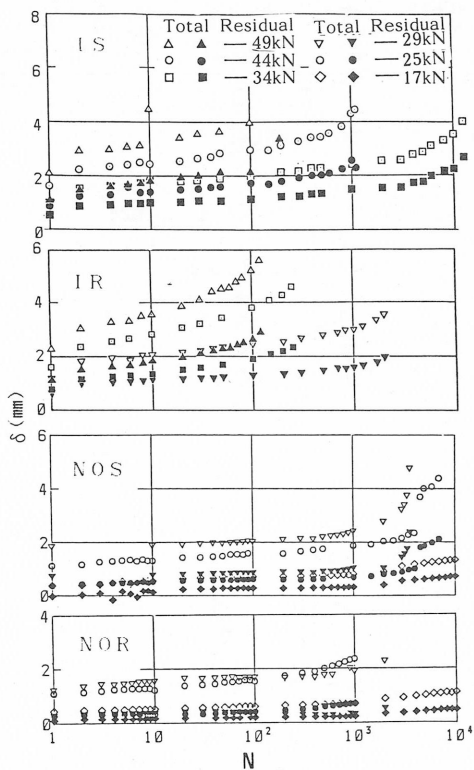


Figure 9 Relation of the repetitive number ( $N$ ) of tracking and central deflection ( $\delta$ )

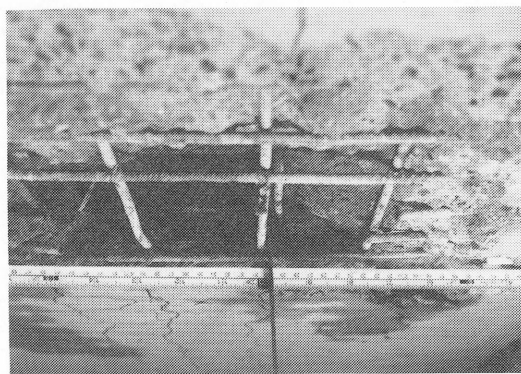


Photo 2 Fatigue section

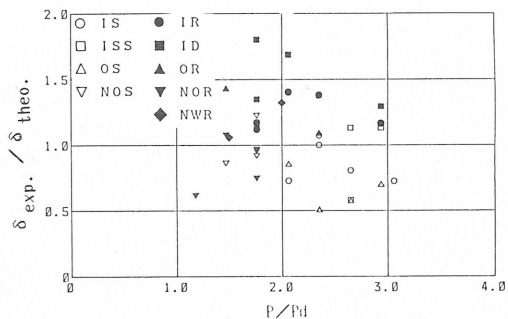


Figure 10 Ratio of elastic deflection to theoretical value at just before collapse

On the other hand, in slab NOR with top reinforcements, cracks (width 0.05–0.15 mm), on the top surface as well as the bottom surface of slab initially occurred due to concrete-shrinkage.

Under  $P=24.5\text{kN}$ , as increase of the repetitive number of wheel tracking, cracks on bottom surface spread, and the slab collapsed at  $N=1775$ . Collapse modes of all the slabs were of punching shear. As shown in Photo 2, the failure surface in the direction of the shorter span spread downward in the direction of 45 degree from the edge of the load portion.

### (3) Deflection characteristics

The relation of the repetitive number  $N$  of wheel tracking to deflection at the center of slab is shown in Figure 9. In this figure total deflection means the sum of elastic and residual deflections (plastic deflection). After the first tracking ( $N=1$ ), total deflection amounted to 1.3 times as large as the static deflection (Figure 6). Then both elastic and residual deflections increase gradually according to increase of  $N$ . But the increasing rate of elastic deflection was slow in comparison with that of residual deflection. Total deflection just before collapse amounted to 3-6mm in the test slabs with the shorter span of 80cm. Since those values are smaller than 15-25mm observed in the static test, it may be concluded that tracking of a wheel load is apt to make a shear failure of slab.

For all the tested slabs, the ratio of elastic deflection immediately before collapse to the calculated deflection by an orthotropic elastic plate theory neglecting tensile concrete in slab section is shown in Figure 10. The abscissa in this figure gives the ratio of wheel load to the equivalent design load ( $P_d$ ) mentioned before. The ratio of elastic deflection immediately before collapse to the theoretical value ranges from 0.5 to 1.8, and the average is 1.05 and the dispersion of distribution is 0.09.

On the other hand, as to residual deflection  $\delta$ ,  $\delta - \log N$  curve is almost linear up to a certain repetitive number  $N_s$  of wheel tracking, and after  $N_s$  the gradient is accelerated larger, and the slabs reach to collapse. In behavior of slabs before  $N_s$ , a lot of fine concrete powder and some angular particles from cracks dropped, after  $N_s$  exfoliations of the covering concrete and differences in level between crackings of bottom surface became visible. Namely, it may be regarded that  $N_s$  is corresponding to a transition from a bending cracking stage to a shear cracking stage.

### (4) Strains in reinforcement

Figure 11 shows variation of strains in main and distribution reinforcements at the center of slabs. Under a relatively higher load such that strain in main reinforcements exceeds to the yield point, the strains were increasing as the repetitive number ( $N$ ) of wheel tracking increases and the slabs collapsed at less than several hundreds of  $N$ . On the other hand, under a relatively lower load such that strains in main reinforcements were less than the yield point, the rate of strain increase in main reinforcements was slow and it was similar to that in deflection. In addition, elastic strains in main reinforcements did not exceed to the calculated values by the conventional design equation. On the contrary, strains in distribution reinforcements were very small and they held almost constant or decreased as  $N$  increased.

From the above observation, it can be suggested that after bending cracks parallel to main reinforcements progress soon to the neutral surface of slab, cracks parallel to distribution reinforcements extended, and then the abrasion of crack faces mainly develops according to increase of wheel tracking and causes the degradation of shear resistance of slab.



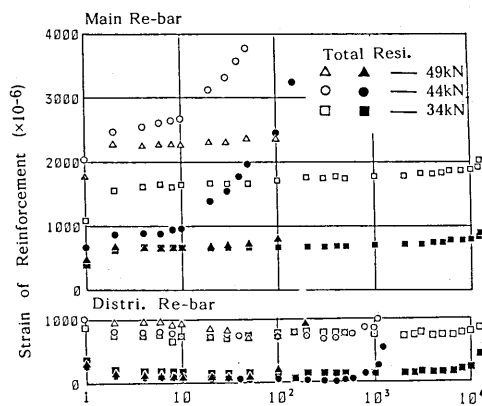


Figure 11 Variation of strain in re-bar

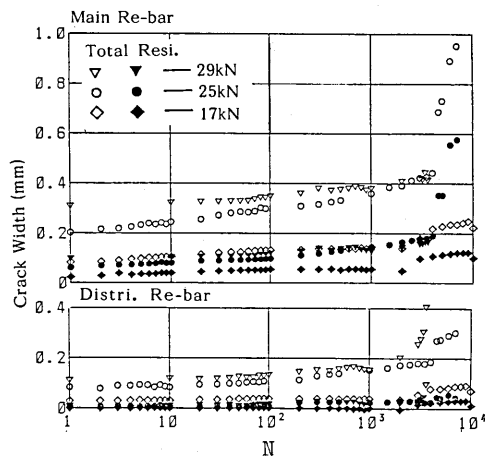


Figure 12 Variation of crack width (slab NOS)

### (5) Crack width

Figure 12 shows variation of crack widths at the center of slab. The crack widths were measured by a pi-shaped extensometer set across a few cracks. Variation of crack widths parallel to distribution reinforcements were similar to that of residual deflection shown in Figure 9. The measured values of crack widths parallel to main reinforcements were small. Considering that visible cracks formed a grid pattern as shown in Figure 8, it can be pointed out that crack widths parallel to main reinforcements were enlarged by making a slit opening due to abrasion of crack faces, which could not appear in the measured value by an extensometer. Such a formation of slit opening was confirmed by falling of fine powder of concrete from cracks of the bottom surface of slab. The fact that the slit came out in cracks parallel to main reinforcements rather than distribution ones may be caused by a beating of crack faces and an alternative action of shearing forces by the repeated passage of wheel load on cracks.

In consequence, it can be mentioned that the slit formation decreases the shear strength of slab which is relying on the interlocking of concrete aggregate and makes redistribution of shearing force to the direction of the shorter span, and eventually a large part of shearing force get to be supported as a beam with a certain effective width.

## 2.4 CONSIDERATIONS

### (1) Cracking damage and fatigue strength

It is generally considered that the degree of cracking damage of RC slab may be evaluated by using the following quantities as a damage index:

- 1) stress intensities of reinforcements under a certain load,
- 2) residual crack widths,
- 3) elastic deflection under a certain load, and
- 4) residual deflection.

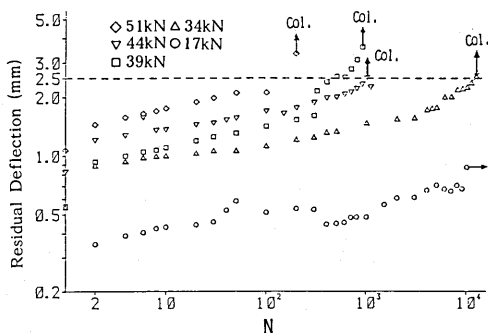


Figure 13 Variation of residual deflection at the center of slab IS

Table 6 Relation of  $\log \delta$  to  $\log N$

	S	A	B	$\log N_{2.5}$	Exp.
I S	0.49	1.375	0.1021	2.54	2.29
	0.42	1.100	0.0969	3.68	3.09
	0.37	0.859	0.1089	4.26	2.99
	0.33	0.747	0.1070	4.90	4.09
	0.16	0.344	0.0707	12.2	—
I R	0.49	1.320	0.1384	2.01	2.10
	0.34	1.011	0.1415	2.78	2.43
	0.29	0.863	0.0983	4.70	3.31
	0.24	0.492	0.1114	6.34	—
	0.16	0.420	0.0896	8.64	—
I D	0.40	1.005	0.1367	2.89	2.57
	0.28	0.642	0.1941	3.04	2.78
	0.24	0.545	0.2379	2.78	2.59
	0.20	0.474	0.8442	10.9	—
	0.14	0.534	0.0714	9.39	—
O S	0.49	1.501	0.0745	2.98	2.29
	0.44	1.075	0.0936	3.91	3.08
	0.39	1.033	0.0651	5.90	3.74
O R	0.50	0.828	0.2625	1.83	1.94
	0.32	0.307	0.2724	3.35	3.04

Since collapse mode is not of a bending type, the stress intensities of reinforcements are not appropriate for a damage index. It is difficult to use residual crack widths as a damage index, because of their large scattering. The increase of elastic deformation means a degradation of stiffness of slab, but it is disadvantageous in accuracy, because of the increase rate of elastic deflection is relatively slow. In consequence, residual (plastic) deflection is most suitable for a damage index, considering that it also has a physical meaning of concerning dissipation energy. Figure 13 shows relations of the residual deflection( $\delta$ ) and the repetitive number( $N$ ) of wheel tracking, which is obtained by rearranging the data in Figure 9 using a bi-logarithmic coordinates.

In the tests of IS, IR, ID, OS, and OR which were made in the same period and had the same concrete strength, the slabs collapsed immediately after the residual deflection reached to a constant value (about 2.5mm). When the residual deflection  $\delta$  is less than 2.5mm, the relation between  $\log \delta$  and  $\log N$  seems to be almost linear, namely

$$\log \delta = \log A + B \log N \quad \dots (1)$$

The coefficients A and B in this equation are obtained by the least square method, as shown in Table 6. In this table, S means the ratio of wheel load to the static collapse load,  $N_{2.5}$  is the repetitive number of wheel tracking corresponding to  $\delta=2.5\text{mm}$  in Eq.(1), and Exp. shows a logarithmic value of N at collapse directly observed in the tests. From this Table, it is pointed out that the fatigue life under the equivalent design load ( $P_d$ ) mentioned before corresponds to  $10^5$ - $10^7$  times that under a load twice as large as  $P_d$ . Conversely, the degree of damage by one tracking ( $N=1$ ) of a load twice as large as  $P_d$  corresponds to  $10^5$ - $10^7$  times that by  $P_d$ . Table 7 shows prediction of the strengths (S) at  $N=1$  and  $N=10^4$ . The value indicated by  $\log N_{2.5}$  are obtained from rearranging the results in Table 6 by equation  $S = A^* + B^* \log N$ . Exp. means the values directly evaluated by the least square method from the data in Figure 7. From these results, it is concluded that the residual strength after first one tracking reduces to 50-80% of static strength.

## (2) Influence of compressive reinforcement for fatigue strength

As mentioned before, the fatigue strength of test slabs with top reinforcements which were placed in the compressive side was less than that of test slabs without top reinforcements. This seems to be caused by the following factors.

- 1) The effective shear section of concrete decreases by an existence of top reinforcements.
- 2) The tensile stresses and initial cracks due to concrete-shrinkage are likely to arise by the restriction of top reinforcements.

Penetrated cracks through the whole section of slab may easily occur by the restriction of reinforcements in both the tensile and compressive sides. In slabs with penetrated cracks, therefore, it is supposed that the abrasion of crack faces are accelerated by the repetition of wheel tracking, and the shear resistance of slab rapidly decreases.

### (3) Mechanism of fatigue collapse

Under tracking of a relatively large load, main reinforcements yielded and the slabs collapsed at less than several hundreds of repetition of wheel tracking. On the other hand, under tracking of a relatively small load less than twice as large as the equivalent design load ( $P_d$ ), the reinforcements of slab did not yield and their strains held almost constant, and the slabs approached to collapse with the growth of deflection and the extension of cracks. Bending fracture of slab under repeatedly moving loads, theoretically, may be considered as an incremental collapse or a cyclic plastic collapse. Collapse at a small number of repetition of wheel tracking seems to be mainly controlled by an incremental collapse.

E.Melan assumed that a slab would arrive at the stage of shakedown in which an elastic behavior repeated only, if a total moment  $M_{sij} + M_{rij}$ , which was composed with an elastic moment  $M_{sij}$  occurred under repetition of wheel load and residual moment  $M_{rij}$  to be independent for time did not violate a yield condition according to E.Melan's theory, a slab will shake down so as to behave elastically after a certain plastic deformation ceases, if a total moment  $M_{sij} + M_{rij}$ , in which  $M_{sij}$  is an elastic moment occurred by a moving load  $P$  and  $M_{rij}$  is a residual moment independent on time, does not violate a yield condition in a whole domain of the slab. Then determining shakedown load ( $P_{sd}$ ) will be reduced to the following problem:

$$P_{sd} = \text{maximize } P$$

$$\text{subject to } f(M_{ex} + M_{rx}, M_{ey} + M_{ry}, M_{exy} + M_{rxy}) = 0 \quad \dots (2)$$

where function  $f$  is yield condition.

Although all test slabs are of finite rectangular plate with all simply supported edges, the slabs may be regarded as an one-way slab, because a wheel load on the slab repeatedly moves over enough long distance in the direction of longer span and shear failure by twisting moment at the corners of the slabs is prevented.

Since a residual moment yielded under such a loading condition diminishes by virtue of structural symmetry and simply supported condition at the edges. Eq.(2) can be reduced to:

$$P_{sd} = \text{maximize } P$$

$$\text{subject to } f(M_{ex}, M_{ey}, M_{exy}) = 0 \quad \dots (3)$$

Solution  $P_{sd}$  of Eq.(3) equals to an elastic limit load when load  $P$  is applied at the slab center. It is conversely suggested that such a load corresponds to  $P_{sd}$  when the maximum value of elastic principal moment of the slab is equal to the ultimate moment  $M_u$  of cross section.

Shakedown load  $P_{sd}$  for each slab is listed in Table 8 from using the ultimate moment  $M_u$  given by the Standard Specification for Design and Construction of Concrete Structure in Japan [1].

If theoretical stresses in distribution reinforcement are less than those in main reinforcement, load  $P_{sd}$  may be governed by the ultimate moment in the direction of distribution reinforcement. For this case, however, load  $P_{sd}$  is still based on the ultimate moment in the direction of main reinforcement, because the magnitude of actual stresses in distribution reinforcement is very small than that in main reinforcement as known in the experimental results already obtained.

Comparing the test results in Figure 7 and the theoretical results in Table 8, we can derive the following discussion: One of the reason why the fatigue strength of test slab ISS with the larger strength of reinforcement was larger than other slabs, may depend on the effect of larger incremental collapse load, namely larger shakedown load. On the other hand, the fracture of slab under tracking of a smaller load than shakedown load may be due to a shear fracture of concrete. As mentioned before, after the development of bending cracks, the crack faces especially parallel to main reinforcements rub out by the repetition of wheel tracking. Therefore, it is supposed that a mechanism supporting shearing forces of a slab varies to that as a beam with a span equal to the shorter span of slab.

Now, consider that a simple beam with a certain effective width carries the whole shearing force. Then, the effective width may be defined as follows:

$$b_e(x) = \frac{2}{Q_{x0}} \int_0^{b/2} Q_x dy \quad \dots (4)$$

in which x-axis is taken from the center of slab in the direction of the shorter span, y-axis (normal to x-axis) is taken in the direction of the longer span,  $Q_x$  is shearing force on slab section facing to x-axis,  $Q_{x0}$  is the value of  $Q_x$  at  $y=0$  and  $b$  is slab width.

If  $b$  is enough large to the shorter span ( $a$ ),  $b_e(x)$  in Eq.(4) reduces to  $P/2Q_{x0}$ , where  $P$  is the intensity of wheel load at the center of slab. The  $b_e(x)$  is a function of  $x$ , and takes the minimum value at  $x=u/2$  ( $u$  is width of wheel loaded portion), and the maximum value at  $x=a/2$ . In the fatigue tests described before, the fracture surface spread downward in the direction of 45 degree from the edge of wheel loaded portion. Then, assuming that  $x=u/2+d$  ( $d$  is effective depth) is critical point for a shear fracture, the effective width for shear resistance is defined as follows.

$$b_{e0} = b_e \left( \frac{u}{2} + d \right) \quad \dots (5)$$

Setting the contact area of a wheel as  $u \times v=15\text{cm} \times 5\text{cm}$ , and  $d=6.0\text{--}6.5\text{cm}$  for each test slab, Eqs.(4) and (5) give  $b_{e0}=0.37\text{--}0.38\text{m}$  using a thin elastic plate theory. According to the Standard Specification for Design and Construction of Concrete Structure in Japan [1], the shear fatigue strength of RC beam without shear reinforcements is given as follows:

$$V_{rcd} = V_{cd} \left( 1 - \frac{\log N}{11} \right) \quad \dots (6)$$

where  $V_{cd} = 0.9\beta_d \cdot \beta_p \cdot \beta_n \cdot b_{e0} \cdot d \cdot \sqrt[3]{f'_{cd}}$ ,  $\beta_d = \sqrt[4]{100/d}$ ,  $\beta_p = \sqrt[3]{100p}$ ,  $\beta_n = 1$   
in which  $f'_{cd}$  is compressive strength of concrete,  $p$  is reinforcement ratio.

Static shear strengths ( $P_{so}=2V_{cd}$ ) of the test slabs obtained by Eq.(6) are and shakedown load ( $P_{sd}$ ) are shown in Table 8.

For all the collapse slabs, relationships between the fatigue lives ( $N$ ) and the ratio ( $S$ ) of the applied wheel load ( $P_f$ ) to the static shear strength ( $P_{so}$ ) are shown in Figure 14, in comparison with the values predicted by the following equation [1] :

$$P_f = P_{so} \left( 1 - \frac{\log N}{11} \right) \quad \dots\dots (7)$$

Table 7 Strengths at  $N=1$  and  $N=10^4$       Table 8  $P_{sd}$  and  $P_{so}$  for each test slab

	Crite- rion	S (N=1)	S (N=10 <sup>4</sup> )	A*	B*
IS	logN <sub>2.s</sub>	0.5253	0.4011	0.5253	-0.0311
	Exp.	0.6658	0.3277	0.6658	-0.0845
IR	logN <sub>2.s</sub>	0.5139	0.3424	0.5139	-0.0429
	Exp.	0.7468	0.1751	0.7468	-0.1429
OS	logN <sub>2.s</sub>	0.5799	0.4486	0.5799	-0.0328
	Exp.	0.6489	0.3737	0.6489	-0.0688
OR	logN <sub>2.s</sub>	0.7167	0.2430	0.7167	-0.1184
	Exp.	0.8175	0.1629	0.8175	-0.1636

Slab	IS IR ID	ISS	OS OR	NOS NOR	NWR
Psd(kN)	49.2 (49.2)	60.0 (60.0)	23.8 (49.2)	35.7 (45.9)	32.9 (46.0)
Pso(kN)	47.9	37.0	47.9	35.7	36.3

Note) Parenthesis shows the results referred to only the ultimate bending moment in the direction of main re-bar.

Figure 14 includes the results due to Matsui's experiments [8] in a high cycle range. His experiments carried out under a wheel tracking load for simply supported rectangular slabs whose shorter span was 1.8m, width was 3m, slab depth was 19cm, and main reinforcement ratio was 0.013. The collapse mode was similar to that of our experiments. Applying Eqs.(5) and (6) to his slabs, we obtain  $b_{e0}=0.87m$ ,  $P_{sd}=53.6kN$ ,  $P_{so}=24.5-29.4kN$  for slab FA, and  $b_{e0}=0.89m$ ,  $P_{sd}=45.1kN$ ,  $P_{so}=29.4-31.4kN$  for slab FB. From Figure 14, it may be mentioned that Eq.(7) gives a good agreement with the data of all the test slabs except slab ISS with a higher yield point of reinforcements.

### 3. FATIGUE STRENGTH OF RC DECK SLAB OF HIGHWAY BRIDGE

Assuming that Eq.(7) is valid in high cycle range of the repetition of wheel tracking, as it may be supported by Figure 14, one may evaluate the fatigue strengths and lives of RC deck slabs of highway bridge. According to the Standard Specifications of Highway Bridge in Japan, the contact area of rear wheel tire to the surface of deck slab is 50cmx20cm, a distance between adjacent main girders, namely the span of deck slab is 2-3m, and the effective depth of deck slab is 14-22cm.

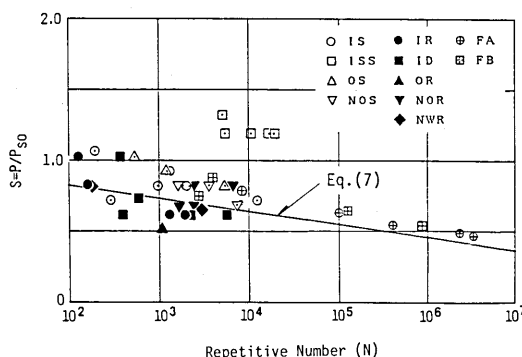


Figure 14 Relation of  
S - log N

Table 9 Values of  $b_{e0}$  (m)  
and  $P_{s0}$  (kN)

d (cm)	$\ell$ (m)					
	2.0		2.5		3.0	
	beo	Pso	beo	Pso	beo	Pso
14	1.02	269	1.05	277	1.06	279
18	1.14	386	1.17	397	1.18	400
22	1.19	490	1.23	496	1.25	504

Table 10 Values of  $P_{s0}$  (kN)  
and  $\log N$

d (cm)	$\ell$ (m)					
	2.0		2.5		3.0	
	Pso	logN	Pso	logN	Pso	logN
14	231	6.53	246	6.79	253	6.91
18	279	7.29	295	7.49	304	7.59
22	302	7.57	321	7.77	332	7.88

Table 9 shows the effective widths by Eq.(5) and the static strengths ( $P_{s0}=2V_{od}$ ) by Eq.(6) for various deck slabs to meet the above specifications, under the assumptions of  $f'_{cd}=23.5\text{MPa}$  and  $p=0.015$ . In Table 9, it can be observed that the effect of the span of slab is rather small, but  $P_{s0}$  is mainly influenced by the effective depth of slab.

According to Eq.(7), the fatigue strength at  $N=2 \times 10^6$  reduces to 43% of static strength. Table 10 shows the fatigue strengths and lives of deck slab when the maximum stress intensity of main reinforcements equals to the allowable tensile stress ( $\sigma_{ca}=137\text{MPa}$ ) specified by the above specifications. From this table, it is observed that among the slabs with the same static strength according to the specifications, fatigue lives become really longer as the depth of slab becomes larger, but they are scarcely influenced by the span of slab.

#### 4. CONCLUSIONS

The conclusions of this study are following:

- 1) All the slabs collapsed in a punching shear mode under both the static and fatigue tests, and any fracture of reinforcements was not associated.
- 2) The fatigue strengths of slabs with the same amount of reinforcements were considerably influenced by slab depth.
- 3) The fatigue lives of slab with compressive reinforcements were shorter than that without them. Main factor of this result seemed to be initial shrinkage cracks in concrete, which were caused by the restriction of both tensile and compressive reinforcements.
- 4) Elastic deflections just before collapse were 0.5-1.8 times (mean 1.05, variance 0.09) as large as theoretical values obtained by an orthotropic thin elastic plate theory neglecting tensile concrete stiffness in slab section.
- 5) The influence of tracking of a wheel load on the strength of slab is very large. Namely, by one tracking of a wheel load the strength of slab reduces to 50-80% of static strength.
- 6) Under the repetition of wheel tracking load twice as large as the equivalent design load, the stresses of main reinforcements did not vary so much, and the stresses of distribution reinforcements were less than values by an ordinary design equation for RC beams.
- 7) The number and width of cracks on the bottom surface of slab grew larger as the repetition of wheel tracking increased. Especially crack widths parallel to main reinforcements increased in association with not only flexural deformation but also the abrasion of crack faces of concrete.
- 8) Slabs with a slit opening at cracks due to the abrasion lost the shearing resistance of slab section normal to distribution reinforcements. Consequently, the mechanism supporting to shearing forces of a slab varied to that as a beam with a certain effective width.

- 9) Calculating the effective width by a thin elastic plate theory and using the shear fatigue strength equation for beams without shear reinforcements which is presented by the Standard Specification for Design and Construction of Concrete Structures in Japan, one can well predict mean values of the fatigue strengths obtained in our experiments in low cycle range of  $N < 10^4$ , and the Matsui's experimental results in a high cycle range of  $N > 10^4$ .
- 10) If the results mentioned above are applied to RC deck slabs of highway bridge, it is found that, for slabs designed by the standard specifications of highway bridge in Japan, the fatigue lives of deck slabs with the same static strength are larger as the effective depth is larger.

## 5. REFERENCES

- [1] Japan Society of Civil Engineer, Standard Specification for Design and Construction of Concrete Structures, 1986.
- [2] Kurata, K., Sonoda, K., Sanematu, H. and Takemura, Y., A consideration for fatigue fracture mechanism and experiments of RC slab already used, Science Council of Japan. The 22nd Symposium of Structural Engineering, pp. 63-70, 1976.
- [3] Okamura, H and Sonoda, K., Mechanical characteristics of cracked slabs, The Kansai Branch of JSCE, The Report of Fatigue Design Committee for RC Slabs "An approach for fatigue design and damage of RC slabs", pp. 75-112, 1977.
- [4] Okada, K., Okamura, H. and Sonoda, K., Fatigue failure mechanism of reinforced concrete bridge deck slabs, Transportation Research Record 664, pp. 136-144, TRB, Washington DC, 1978.
- [5] Okada, K., Okamura, H., Sonoda, K. and Shimada, I., Cracking and fatigue behavior of bridge deck RC slabs, Proceedings of the JSCE, No.321, pp. 49-61, 1982.
- [6] Imai, H., Okada, K., Kojima, T. and Mizumoto, Y., Study on shrinkage cracks in reinforced concrete deck slabs of bridges, Proceedings of the JSCE, No.340, pp. 175-184, 1983.
- [7] Melan, E., Theorie statish unbestimmeter Systeme, Preliminary Publication of 2nd Congress of IABSE, pp. 43-64, Berlin, 1936.
- [8] Matsui, S., Okamura, H., Sonoda, K. and Okada, K., Concepts for deterioration of highway bridge decks and fatigue studies, International Symposium of Fundamental Theory of Reinforced and Prestressed Concrete, Nanjing, China, 1986.